Polystyrene−ZnO Composite Particles with Controlled Morphology

Mukesh Agrawal,*,† Andrij Pich,*,‡ Nick E. Zafeiropoulos,† Smrati Gupta,† Juergen Pionteck,† Frank Simon,† and Manfred Stamm†

Leibniz-Institut für Polymerforschung Dresden e.V., Hohe Strasse 6, 01069 Dresden, Germany, and Technische Universität Dresden, Institut für Makromolekulare Chemie and Textilchemie, Mommsenstrasse 4, 01062 Dresden, Germany

Received November 19, 2006. Revised Manuscript Received January 30, 2007

The present study reports on a versatile method of the preparation of polystyrene−ZnO composite particles with core−shell or raspberry-like morphology. SEM analysis revealed that ZnO has been deposited on the surface of functionalized polystyrene beads as either a continuous thin layer or small clusters, depending on the reaction parameters. We propose that the interaction between ZnO nanoparticles and β-diketone groups, present on the surface of polystyrene beads, is the driving force for the preparation of these composite particles. IR spectroscopy was used to prove the interaction between ZnO nanoparticles and β-diketone groups. X-ray diffraction of the PS/ZnO particles revealed diffraction peaks corresponding to wurtzite ZnO crystalline phase. TGA results demonstrated that the ZnO contents of composite particles can be varied by changing the concentration of $Zn(Ac)_2 \cdot 2H_2O$ salt prior to reaction. The composite particles produced are envisioned to have applications as the building blocks for fabrication of sensors, transducers, actuators, UV detectors, and optoelectronic devices.

Introduction

Semiconductor nanoparticles have been studied intensively because of their potential application in photonic crystals,[1] optical sensitizers, photocatalysts,[2] light converting electrodes,[3] etc. Among all semiconductors, ZnO is a technologically important material exhibiting quantum confinement effects in an experimentally accessible size range. Typical applications of ZnO include sensors, UV light-emitting devices, solar cells, transducers, etc. Numerous efforts have been made to study the precipitation of ZnO in the aqueous phase and control the morphology and physicochemical properties of the formed crystals. The influence of the preparation methods[4−7] as well as the reaction parameters[8,9] (temperature, pH, concentration, and reaction time) on the final properties and morphology of formed ZnO crystals have been studied. A number of research groups have used the block- and graft-copolymers[10,11] or surface-functionalized latex particles[12,13] as additives in the crystallization process to affect the morphology of ZnO crystals. Extensive work has been carried out on the synthesis of ZnO nanoparticles via solution methods, which are usually based on the reaction of various types of zinc salts in alcohol (methanol,[14] ethanol,[15−17] and 2-propanol[18−23]) as well as in aqueous[24] media with NaOH or LiOH as oxygen sources. It has been reported that the nucleation, growth, and final properties of ZnO nanoparticles depend strongly on the reaction temperature and nature of the alcohols or zinc salts used in the preparation process.

In recent years, composite particles fabricated by templating the organic or inorganic cores have been receiving significant attention because they exhibit properties that are substantially different from those of the template cores, such as higher surface area, different surface chemical composi-

* To whom correspondence should be addressed. E-mail: agrawal@ipfdd.de (M.A.); andrij.pich@chemie.tu-dresden.de (A.P.).
† Leibniz-Institut für Polymerforschung Dresden e.V.
‡ Institut für Makromolekulare Chemie and Textilchemie.

(1) Park, W.; King, J. S.; Neff, C. W.; Liddell, C.; Summers, C. J. *Phys. Status Solidi* **2002**, *229*, 949.
(2) Hörner, G.; Johne, P.; Künneth, R.; Twardzik, G.; Roth, H.; Clark, T.; Kirsch, H. *Chem.—Eur. J.* **1999**, *5*, 208.
(3) Gaetzel, M. *Platinum Met. Rev.* **1994**, *38*, 151.
(4) Rodrigues-Paez, J. E.; Caballero, A. C.; Villegas, M.; Moure, C.; Duran, P.; Fernandez, J. F. *J. Eur. Ceram. Soc.* **2001**, *21*, 925.
(5) Almeida de Oliveira, A. P.; Hochepied, J. F.; Gritton, F.; Berger M. H. *Chem. Mater.* **2003**, *15*, 3203.
(6) Andres-Verges, M.; Martinez-Gallego, M. *J. Mater. Sci.* **1992**, *27*, 3756.
(7) Music, S.; Draggcevic, D.; Maljkovic, M.; Popovic, S. *Mater. Chem. Phys.* **2002**, *77*, 521.
(8) Wang, L. N.; Muhammed, M. *J. Mater. Chem.* **1999**, *9*, 2871.
(9) Hu, H. Y.; Wang, H.; Zhang, Y. C.; He, W. L.; Zhu, M. K.; Wang, B.; Yan, H. *Ceram. Int.* **2004**, *30*, 93.
(10) Öner, M.; Norwig, J.; Meyer, W. H.; Wegner, G. *Chem. Mater.* **1998**, *10*, 460.
(11) Taubert, A.; Kubel, C.; Martin, D. C. *J. Phys. Chem. B* **2003**, *107*, 2660.
(12) Wegner, G.; Baum, P.; Müller, M.; Norwig, J.; Landfester, K. *Macromol. Symp.* **2001**, *175*, 349.
(13) Munos-Espi, R.; Qi, Y.; Lieberwirth, I.; Gomez, C. M.; Wegner, G. *Chem.—Eur. J.* **2006**, *12*, 118.
(14) Monticone, S.; Tufeu, R.; Kanaev, A. V. *J. Phys. Chem. B* **1998**, *102*, 2854.
(15) Meulenkamp, E. *J. Phys. Chem. B* **1998**, *102*, 5566.
(16) Hoyer, P.; Weller, H. *J. Phys. Chem.* **1995**, *99*, 14096.
(17) Kamat, P. V.; Patrick, B. *J. Phys. Chem.* **1992**, *96*, 6829−6843.
(18) Bahnemann, D. W.; Kormann, C.; Hoffmann, M. R. *J. Phys. Chem.* **1987**, *91*, 3789.
(19) Spanhel, L.; Anderson, M. A. *J. Am. Chem. Soc.* **1991**, *113*, 2826.
(20) Wong, E. M.; Bonevich, J. E.; Searson, P. C. *J. Phys. Chem. B* **1998**, *102*, 7770.
(21) Wong, E. M.; Hoertz, P.; Liang, C. J.; Shi, B.; Meyer, G. J.; Searson, P. C. *Langmuir* **2001**, *17*, 8362.
(22) Hu, Z.; Oskam, G.; Penn, R. L.; Pesika, N.; Searson, P. C. *J. Phys. Chem. B* **2003**, *107*, 3124.
(23) Hu, Z.; Escamilla Ramirez, D. J.; Heredia Cervera, B. E.; Oskam, G.; Searson, P. C. *J. Phys. Chem. B* **2005**, *109*, 11209.
(24) Zhang, S. C.; Li, X. G. *Colloids Surf., A* **2003**, *226*, 35.

10.1021/cm062757g CCC: $37.00
Published on Web 02/23/2007

tion, increased stability, and different magnetic and optical properties. These properties turn the composite particles suitable for a wide range of applications such as surface-enhanced Raman scattering (SERS),[25] catalysis,[26] biochemistry,[27] nonlinear optics, bioanalysis, and capsules for controlled release of therapeutic agents.[28] Polystyrene beads have been reported to serve as an effective template for the preparation of core−shell composite particles, because of their simple preparation, ease in surface functionalization, and flexibility in size variations. Tissot et al.[29,30] reported on the deposition of silica layer on polystyrene latex particles, using a silane coupling agent to compatibilize core and shell materials. Sherman et al.[31] described the coating of cadmium sulfide and cadmium selenide/cadmium sulfide core−shell particles on the polystyrene core, using the electrostatic interaction between core and shell. Chen et al.[32] and Zhong et al.[33] have successfully coated polystyrene beads with inorganic shells composed of silica and titanium-(di)oxide respectively. Apart from direct coating, polyelectrolytes have also been used to facilitate the deposition of nanoparticles on polystyrene beads. For example, Caruso et al.[34,35] recently described the deposition of magnetic and silica nanoparticles on polystyrene microspheres through a layer-by-layer (LBL) deposition method using polyelectrolytes as controlling media. Similarly, Valtchev[36] reported the adsorption of a zeolite layer on polystyrene beads by the combination of LBL and hydrothermal synthesis methods. At the same time, extensive work has been done to synthesize ZnO shells on suitable inorganic cores. Park et al.[37] have prepared ZnO shell on SnO and TiO_2 cores, which can be used for the fabrication of dye-sensitized solar cells. Xia et al.[38] described the preparation of a ZnO layer on silica spheres via the controlled precipitation of the ZnO nanoparticles from $Zn(Ac)_2$ salt in the presence of triethanolamine. On the other hand, Dhas and co-workers[39] reported the sonochemistry as an alternative method for the synthesis of ZnS semiconductor nanoparticles on submicrometer-sized silica by ultrasound irradiation near room temperature.

In the present study, we report on the preparation of polystyrene−ZnO (PS−ZnO) composite particles with effective control over their morphology. The interest arises from the versatility of the system to produce the PS−ZnO composite particles of two different morphologies (core−shell and raspberry-like) by controlling critical reaction parameters. Additionally, this system provides flexibility in size variation, ZnO content, and shell thickness (in case of core−shell particles) of composite particles. PS/ZnO particles with core−shell morphology can be used as building blocks for the fabrication of ZnO based sensors, transducers, actuators, UV detectors, and optoelectronic devices, because of their simple synthesis, nanoscopic dimensions, homogeneous particle size distribution, and flexible adjustment of the size and ZnO content. Moreover, such supported nanostructured materials are very promising for applications in catalysis because they enable a fine dispersion and stabilization of small metallic particles and provide access to a larger number of active sites than the corresponding bulk components. In addition, PS/ZnO composite particles could also be used in the fabrication of photonic crystals similar to the ZnO colloid particles reported by Seelig et al.[40]

On the other hand, particles with a raspberry-like morphology can find application as a carrier of ZnO nanoparticles into suitable polymer matrices to obtain ZnO nanocomposites with better dispersion. Moreover, annealing a film of such raspberry-like particles on a substrate such as glass or quartz at suitable temperature (110 °C) can result in the formation of nanocomposite film with a good dispersion of ZnO nanoparticles in polystyrene matrix. A significant amount of work has already been done on the film formation using latex particles.[41−43]

Table 1. Ingredients Used for the Synthesis of Polystyrene Beads and Their Size

sample	ST (g)	AAEM (wt % ST)	SPDS (g)	water (g)	solid content (%)	size of PS beads (nm)
A	20	1	0.3	180	9.9	650
B	19	5	0.3	180	10.2	540
C	18	10	0.3	180	9.5	300

Experimental Section

Materials. Styrene (ST) (Fluka) and acetoacetoxyethyl methacrylate (AAEM) (97%) (Aldrich) were passed through the inhibitor removal column and then vacuum distilled under nitrogen. Sodium peroxydisulfate (SPDS) (97%), zinc acetate dihydrate ($Zn(Ac)_2 \cdot 2H_2O$) (99%), 2-propanol (99.5%), and ethanol (99%) were all purchased from Aldrich and have been used without additional purification. DMSO (dimethylsulphoxide) and NaOH (98%) were obtained from Fluka and used as received. Distilled water was employed as the polymerization medium.

Synthesis of Polystyrene Particles. Functionalized polystyrene particles with three different sizes (PS-A, 650 nm; PS-B, 540 nm; and PS-C, 300 nm) were prepared by surfactant-free emulsion polymerization. A double-wall glass reactor equipped with a mechanical stirrer and a reflux condenser was purged with nitrogen. Water (170 g) and appropriate amounts of ST and AAEM (see Table 1) were added into the reactor and the reaction mixture was

(25) Cheng, W.; Dong, S.; Wang, E. *J. Phys. Chem. B* **2004**, *108*, 19146.
(26) Chen, C. W.; Serizawa, T.; Akashi, M. *Chem. Mater.* **1999**, *11*, 1381.
(27) Siiman, O.; Burshteyn, A. *J. Phys. Chem. B* **2000**, *104*, 9795.
(28) Lu, C.; Wu, N.; Jiao, X.; Luo, C.; Cao, W. *Chem. Commun.* **2003**, 1056.
(29) Tissot, I.; Novat, C.; Lefebvre, F.; Bourgeat-Lami, E. *Macromolecules* **2001**, *34*, 5737.
(30) Tissot, I.; Reymond, J. P.; Lefebvre, F.; Bourgeat-Lami, E. *Chem. Mater.* **2002**, *14*, 1325.
(31) Sherman, R. L.; Ford, W. T. *Langmuir* **2005**, *21*, 5218−5222.
(32) Chen M.; Zhou S.; Wu L.; Xie S.; Chen Y. *Macromol. Chem. Phys.* **2005**, 206, 1896.
(33) Zhong, Z.; Yin, Y.; Gates, B.; Xia, Y. *Adv. Mater.* **2000**, *12*, 206−209.
(34) Caruso, F.; Spasova, M.; Susha, A.; Giersig, M.; Caruso, R. A. *Chem. Mater.* **2001**, *13*, 109−116.
(35) Caruso, F.; Caruso, R. A.; Mohwald, H. *Chem. Mater.* **1999**, *11*, 3309−3314.
(36) Valtchev, V. *Chem. Mater.* **2002**, *14*, 956−958.
(37) Park, N.-G.; Kang, M. G.; Kim, K. M.; Ryu, K. S.; Chang, S. H.; Kim, D.-K. *Langmuir* **2004**, *20*, 4246−4253.
(38) Xia, H.-L.; Tang, F. -Q. *J. Phys. Chem. B* **2003**, *107*, 9175−9178.
(39) Dhas, N. A.; Zaban, A.; Gedanken, A. *Chem. Mater.* **1999**, *11*, 806−813.
(40) Seelig, E. W.; Tang, B.; Yamilov, A.; Cao, H.; Chang, R. P. H. *Mater. Chem. Phys.* **2003**, *80*, 257−263.
(41) Ugur, S.; Salman, O.U.; Tepehan, G.; Tepehan, F.; Pekcan, Ö. *Polym. Compos.* **2005**, *26* (3), 352.
(42) Ugur, S.; Elaissari, A.; Pekcan, Ö. *Polym. Adv. Technol.* **2005**, *16*, 405−412
(43) Juhue, D.; Lang, J. *Macromolecules* **1995**, *28*, 1306−1308.

Table 2. Variation in Reaction Parameters during Preparation of ZnO Nanoparticles and PS/ZnO Composite Particles

reaction set	*T* (°C)	NaOH conc. (M)	$Zn(Ac)_2 \cdot 2H_2O$ conc. (mM)
1	55	0.2, 0.5, 1, 2[a]	1
2	20,[a] 40, 55, 70	1	1
3[b]	55	0.2	0.5, 1, 1.5, 2

[a] Reaction parameters varied during the synthesis of ZnO nanoparticles only. [b] Reaction set run during the synthesis of PS/ZnO composite particles only.

stirred for 10 min at room temperature. Subsequently, the temperature was raised to 70 °C, and an aqueous solution of SPDS initiator (0.3 g in 10 g of water) was added into the reaction mixture to initiate the polymerization process; the reaction was allowed to proceed for another 24 h at 70 °C. Finally, polystyrene latex particles were obtained as a stable dispersion in water with ca. 10% solid content.

Synthesis of ZnO Nanoparticles and PS−ZnO Composite Particles. A given amount of $Zn(Ac)_2 \cdot 2H_2O$ salt (from reaction set 3 in Table 2) was added to 80 mL of 2-propanol and the mixture was stirred vigorously at 20 °C for 10 min. The reaction temperature was increased to 55 °C and the solution was stirred for another 1 h to dissolve the $Zn(Ac)_2 \cdot 2H_2O$ salt in 2-propanol. For the preparation of PS−ZnO composite particles, 5 g of a dispersion of polystyrene latex particles (with 10% solid content) prepared as above was added to the reaction mixture at this stage, followed by vigorous stirring for 20 min. Subsequently, the reaction mixture was cooled to 20 °C followed by the addition of 2 mL of an aqueous NaOH solution of a set concentration (shown in reaction set 1 from Table 2) dropwise for 8−10 min. Afterward, the reaction mixture was stirred for another 20 min at a given temperature (shown in reaction set 2 from Table 2). Finally, the solution was cooled to 20 °C and the solvent was removed via rotary evaporation at 55 °C. The obtained ZnO powder (PS/ZnO powder in the case of composite particle formation) was washed 3 times with distilled water via centrifugation and dried in a vacuum oven at 20 °C.

Characterization Methods. For the determination of the particle size a commercial laser light scattering (LLS) spectrometer (ALV/DLS/SLS-5000) equipped with an ALV-5000/EPP multiple digital time correlator and laser goniometer system ALV/CGS-8F S/N 025 was used with a helium-neon laser (Uniphase 1145P, output power of 22 mW and wavelength of 632.8 nm) as the light source. IR spectra were recorded with Mattson Instruments Research Series 1 FTIR spectrometer. Prior to analysis, dried samples were mixed with KBr and pressed to form a tablet. Thermogravimetric analysis (TGA) was performed on a TGA 7 (Perkin-Elmer) analyzer. Samples were heated in platinum crucibles in the 25−700 °C temperature range with nitrogen carrier gas at a 5 K/min heating rate. Transmission electron microscopy (TEM) images were recorded on a Zeiss Omega 912 microscope at 160 kV. Scanning electron microscopy (SEM) images were taken on a Gemini microscope (Zeiss, Germany) at an accelerating voltage of 4 V. Samples were prepared by drying a few drops of the samples on aluminum support at room temperature. Samples were coated with a thin Au/Pd layer to increase the contrast and quality of the images. XRD spectra were taken by analyzing the powdery samples on a HZG 4/A-2 (Seifert FPM) X-ray diffractometer.

Results

Polymeric Core Particles. Polystyrene (PS) beads containing the β-diketone groups on their surfaces were prepared by a surfactant-free copolymerization of styrene (ST) and acetoacetoxyethyl methacrylate (AAEM).[44] Because of its hydrophilic character, AAEM is predominantly located on the particle surface after the copolymerization process with styrene and stabilizes the obtained colloidal system. Moreover, this system allows effective control of the particle size of the polystyrene beads by changing the amount of AAEM in the reaction mixture. Figure 1 shows the SEM images of PS beads prepared at different AAEM contents, indicating a gradual decrease in their size with an increase in AAEM content. These images reveal the homogeneous particle size distribution in all three cases and hence decline the possibilities of the formation of poly(AAEM) particles in the system.

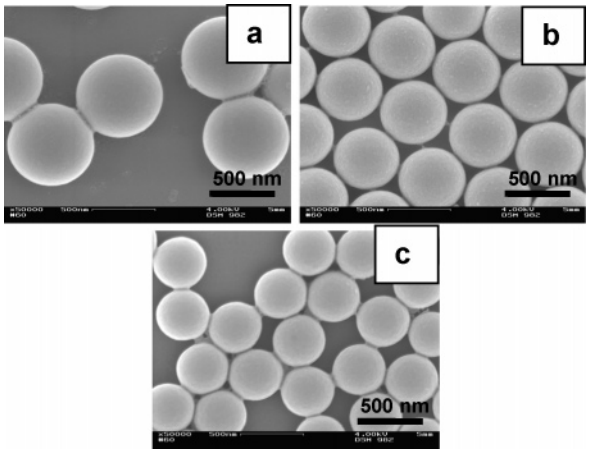

Figure 1. SEM images of Polystyrene particles prepared by using different AAEM contents: (a)1 mol % (PS-A); (b) 5 mol % (PS-B); and (c) 10 mol % (PS-C).

In the present study, PS beads with an average diameter of 540 nm have been used as the templates for the deposition of ZnO nanoparticles. These polystyrene beads have been successfully used in our previous investigations for the deposition of maghemite[45] and zinc sulfide[46] nanoparticles.

PS−ZnO Composite Particles. PS/ZnO composite particles were prepared by templating the ZnO nanoparticles against the functionalized polymeric core. For this purpose, ZnO nanoparticles were synthesized using the Hu et al.[23] method in the presence of polystyrene beads. Interaction between β-diketone groups, present on the template surface, and ZnO precursors is considered to be the driving force for the formation of these PS/ZnO composite particles. Because the Hu et al.[23] method was found to be very effective for coating the PS core with ZnO nanoparticles in our system; therefore, first some reaction sets were run only for the synthesis of ZnO nanoparticles using the Hu et al.[23] procedure. Our aim was to study the effect of different reaction parameters on reaction rate and size of ZnO nanoparticles to optimize the coating of PS beads with ZnO nanoparticles. In this approach, $Zn(Ac)_2 \cdot 2H_2O$ salt was hydrolyzed in the presence of aqeuous NaOH solution in 2-propanol. The concentration of NaOH solution and reaction temperature both were found to affect the reaction rate as well as the particle size and morphology to a great extent.

(44) Pich, A.; Bhattacharya, S.; Adler, H.-J. P. *Polymer*, **2005**, *46*, 1077.
(45) Choi, H.-J.; Jang, L. B.; Lee, J. Y.; Pich, A.; Bhattacharya, S.; Adler, H.-J. P. *IEEE Trans. Magn.* **2005**, *41/10*, 3448.
(46) Pich, A.; Hain, J.; Prots, Yu.; Adler, H.-J. P. *Polymer* **2005**, *46*, 7931.

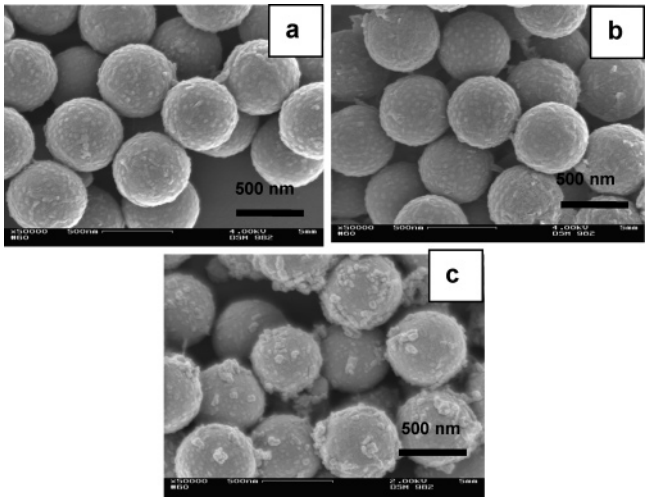

Figure 2. SEM images of PS/ZnO composite particles prepared by using 1 mM $Zn(Ac)_2 \cdot 2H_2O$ conc. at 55 °C and different NaOH concentrations: (a) 0.2, (b) 0.5, and (c) 1 M.

An increase in the reaction temperature (from 20 to 70 °C) and NaOH concentration (from 0.5 to 2 M) led to an increase in nucleation and growth rates of ZnO nanoparticles and induced the particle coarsening effect. Consequently, an acceleration in reaction rate and an increase in particle size were observed (see the Supporting Information, Figures S1 and S2).

According to the literature,[22,23] the preparation of ZnO nanoparticles consists of three different steps: (a) the formation of positively charged complexes in a reaction medium that act as the precursor for ZnO nanoparticles, (b) nucleation and growth processes of ZnO nanoparticles, and (c) coarsening of particles (if reaction conditions are favorable). Therefore, it is believed that during the formation of composite particles, ZnO precursors (positively charged complexes), formed in reaction media, interact with β-diketone groups (which are present on the surface of polystyrene beads) and provoke the nucleation of the ZnO nanoparticles on the surface of PS beads. This nucleation process is followed by growth of formed nuclei until the super saturation state is achieved. To investigate the effect of various reaction parameters on the morphology and ZnO content of composite particles, we synthesized samples following three different reaction sets (shown in Table 2).

Effect of NaOH Concentration. Because the NaOH concentration influences the nucleation and growth processes of ZnO nanoparticles in the reaction media to a great extent, it is also expected to unavoidably have some impact on the coating of the polystyrene beads with ZnO nanoparticles during the formation of composite particles. Figure 2 shows the SEM images of the composite particles, prepared at different NaOH concentrations (from reaction set 1 in Table 2). These images demonstrate that lower NaOH concentrations (0.2 M; 05 M) are favorable for the preparation of PS/ZnO composite particles with core−shell morphology, whereas increasing the NaOH concentration to 1 M results in the formation of raspberry-like composite particles with discrete distribution of relatively large agglomerates of ZnO nanoparticles on the surface of polystyrene beads. This change in morphology with increasing

Table 3. Variation in ZnO Contents of PS/ZnO Composite Particles with $Zn(Ac)_2 \cdot 2H_2O$ and NaOH Concentrations

		ZnO contents (%)	
S.N.	$Zn(Ac)_2 \cdot 2H_2O$ conc. (mM)	at 0.2 M NaOH	at 1 M NaOH
1	0.25	5.39	5.42
2	0.5	5.55	9.62
3	1	7.49	16.79
4	1.5	9.20	17.34
5	2	11	18.29

NaOH concentration can be explained as follows: As reported by Hu et al.,[22] at given reaction conditions, an increase in NaOH concentration in the reaction mixture increases the rates of nucleation and growth of ZnO nanoparticles significantly. Consequently most of the ZnO precursors begin to nucleate in the reaction media, before establishing interactions with functionalized polymer surfaces. In other words, nucleation of ZnO particles on polymer beads (heterogeneous nucleation) is dominated by the one in reaction solution (homogeneous nucleation). Thus, only a fraction of the active sites (β-diketone groups) available on the template surface is used during the ZnO nucleation. Once nucleation is established, the nanoparticles grow rapidly until the super saturation state is achieved, leading to a raspberry-like morphology of composite particles. Moreover, it has also been reported that increasing the NaOH concentration induces a coarsening effect of ZnO nanoparticles because of the increase in solubility of zinc species in the reaction media. Coarsening is a process that involves the growth of larger particles at the expense of smaller particles, which further increases with increasing hydroxyl ion concentration in reaction media. Therefore, at higher NaOH concentration (1 M), one can expect the deposition of islands of relatively larger ZnO nanoparticles on the surface of templates leading to the raspberry-like morphology. In contrast, at lower NaOH concentrations (0.2 and 0.5 M), a slow nucleation and growth processes of ZnO particles as well as a suppressed coarsening effect allow the formation of a continuous ZnO shell on the surface of polymeric core resulting into a core−shell morphology.

Because increasing the NaOH concentration accelerates the hydrolysis of $Zn(Ac)_2 \cdot 2H_2O$ salt, a higher amount of ZnO will be formed and deposited on the polystyrene beads at a given reaction time. TGA results shown in Table 3 confirm this fact, demonstrating the increase in ZnO content of composite particles with increasing NaOH concentration (from 0.2 to 1 M) at the given $Zn(Ac)_2 \cdot 2H_2O$ concentrations.

Effect of Reaction Temperature. To investigate the effect of reaction temperature on the morphology of formed PS−ZnO composite particles, we carried out the synthesis at three different temperatures (from reaction set 2 in Table 2). Figure 3 reveals that the morphology of composite particles changes from core−shell to raspberry-like with increasing reaction temperature (from 40 to 70 °C), similar to the effect of the NaOH concentration. This can also be attributed to the acceleration of the nucleation and growth rates of ZnO particles (because of a decrease in their activation energies) as well as an induced coarsening effect at higher reaction temperatures (55 and 70 °C). Increasing the reaction temperature causes the solubility of zinc species in the reaction media to also increase (as reported by Hu et al.[23]), which in

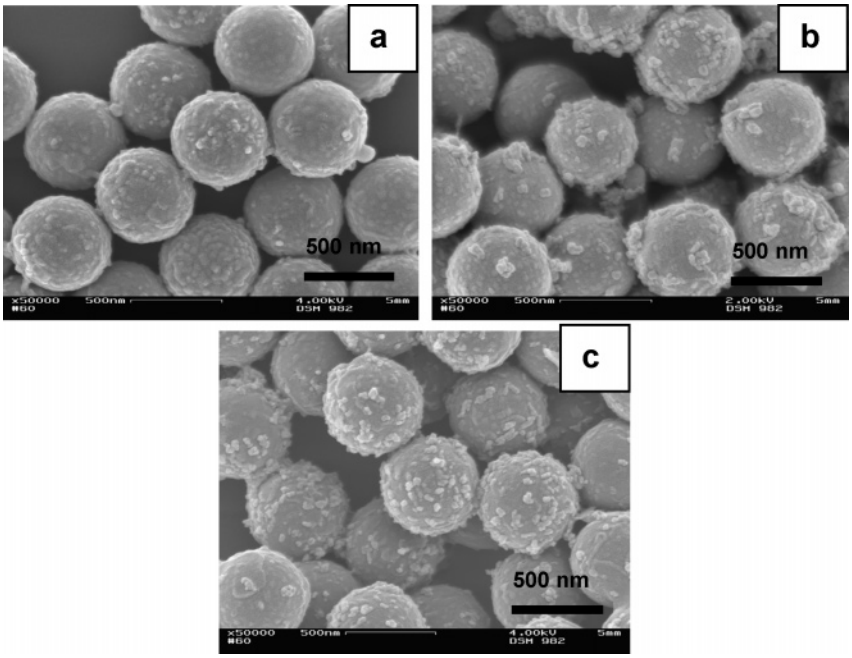

Figure 3. SEM images of PS/ZnO composite particles prepared by using 1 mM $Zn(Ac)_2 \cdot 2H_2O$ conc. and 1 M NaOH conc. at different reaction temperatures: (a) 40, (b) 55, and (c) 70 °C.

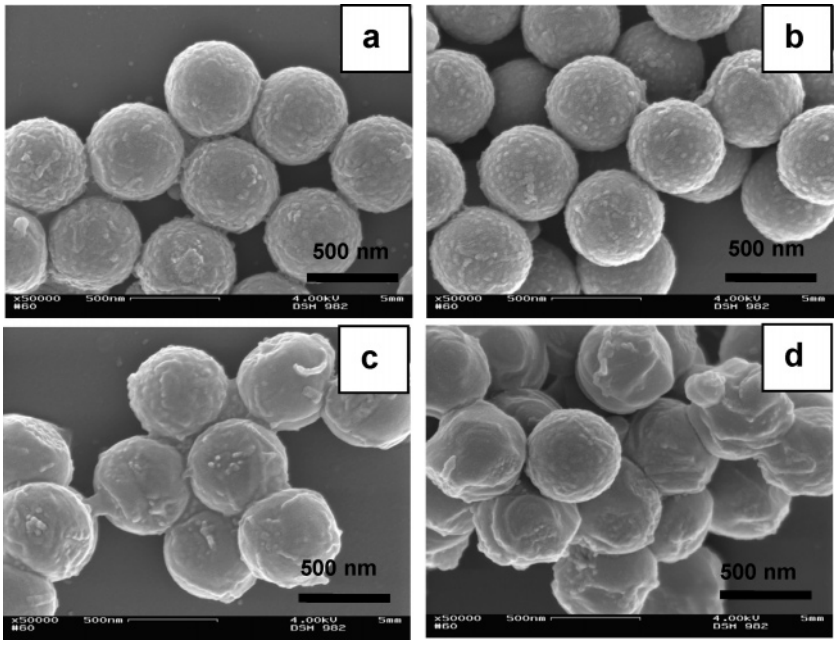

Figure 4. SEM images of PS/ZnO composite particles prepared by using different $Zn(Ac)_2 \cdot 2H_2O$ concentrations: (a) 0.5, (b) 1, (c) 1.5, and (d) 2 mM at 0.2 M NaOH conc. and 55 °C temperature.

turn enhances the coarsening-effect of ZnO particles and consequently leads to the deposition of large aggregates on the template surface.

Effect of $Zn(Ac)_2 \cdot 2H_2O$ Concentration. Figure-4 illustrates SEM images of composite particles prepared at different $Zn(Ac)_2 \cdot 2H_2O$ concentrations (from set 3 in Table 2). From these images, one can observe the typical core−shell morphology of composite particles in all cases. These results reveal that composite particles are smooth in surface and uniform in size at lower $Zn(Ac)_2 \cdot 2H_2O$ concentrations (0.5 and 1 mM), suggesting the formation of a well-defined ZnO layer on polymer beads. On the other hand, increasing the concentration to 1.5 and 2 mM causes the deposition of a large amount of ZnO nanoparticles, which results in deviation from the spherical shape of the composite particles. The higher the $Zn(Ac)_2 \cdot 2H_2O$ concentration in the mixtures, the larger the number of ZnO precursors (zinc ions) produced in the reaction medium to interact with active sites of polymer beads; therefore, an increased amount of ZnO nanoparticles will be deposited on the PS beads.

TGA results shown in Table 3 illustrate the variation in ZnO content for the composite particles with respect to the amount of $Zn(Ac)_2 \cdot 2H_2O$ salt at two different NaOH concentrations. These results reveal that when the synthesis is carried out at 0.2 M NaOH, the ZnO content increases in a linear fashion with the change in $Zn(Ac)_2 \cdot 2H_2O$ concentration from 0.5 to 2 mM, whereas if the same effect is studied on the 1 mM NaOH, the ZnO content increases linearly up

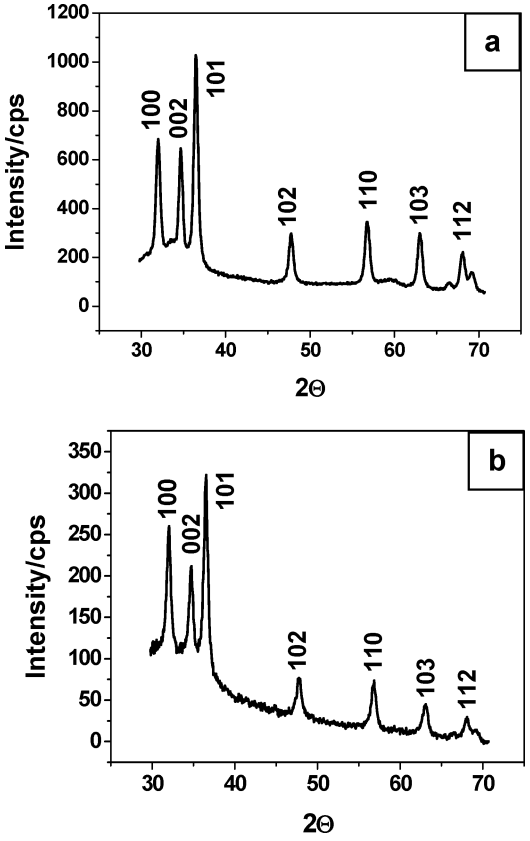

Figure 5. XRD spectra of (a) ZnO nanoparticles and (b) PS/ZnO composite particles prepared by using 1 mM $Zn(Ac)_2 \cdot 2H_2O$ at 1 M NaOH conc. and 55 °C temperature.

to only a 1 mM concentration of $Zn(Ac)_2 \cdot 2H_2O$ salt. A further increase in the zinc salt concentration causes only a slight increment in ZnO contents. As explained above, 0.2 M NaOH concentration is the most favorable parameter for heterogeneously precipitating ZnO particles; therefore, an increase in the $Zn(Ac)_2 \cdot 2H_2O$ amount at this NaOH concentration will result in a linearly increasing ZnO content of composite particles. On the other hand, at a 1 M NaOH concentration, homogeneous precipitation of ZnO particles comes into action to a great extent, and hence increasing the $Zn(Ac)_2 \cdot 2H_2O$ concentration above a certain value at this NaOH concentration results in insignificant changes in the amount of ZnO nanoparticles deposited on polystyrene beads.

Figure 5 shows the XRD patterns of ZnO nanoparticles, prepared by the Hu et al.[23] method and PS/ZnO composite particles. The diffraction patterns of synthesized ZnO nanoparticles and composite particles exhibit the characteristic peaks for crystalline ZnO of wurtzite structure and confirm the purity and crystalline nature of ZnO nanoparticles deposited on the polymer core. The diffraction peaks can be indexed to the hexagonally structured ZnO with cell constants of $a = 0.324$ nm and $c = 0.519$ nm, which are consistent with the standard values for bulk ZnO (JCPDS card 36-1451).

IR spectroscopy was used to confirm the interaction of ZnO nanoparticles with β-diketone groups, located on the surface of polystyrene beads. Figure 6 shows IR spectra of PS−ZnO samples prepared using different $Zn(Ac)_2 \cdot 2H_2O$ concentrations at 0.2 M NaOH. It may be seen that increasing the ZnO content in the composite particles, with increasing

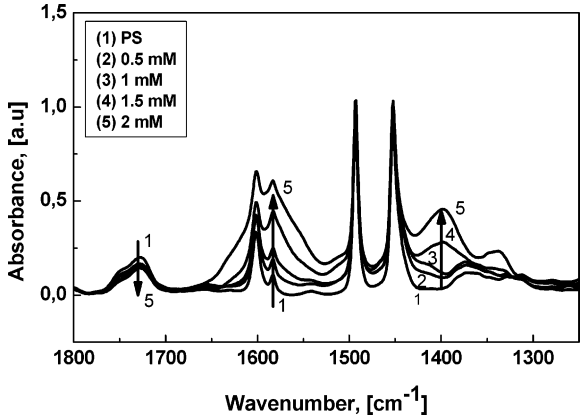

Figure 6. IR spectra of PS/ZnO composite particles prepared using different $Zn(Ac)_2 \cdot 2H_2O$ concentrations: (1) 0, (2) 0.5, (3) 1, (4) 1.5, and (5) 2 mM at 55 °C and 0.2 M NaOH (final ZnO content: (1) 0, (2) 5.4, (3) 7.49, (4) 9.2, and (5) 11%).

$Zn(Ac)_2 \cdot 2H_2O$ concentration (as confirmed by TGA results shown in Table 3) led to the appearance of the C═O stretching band at 1584 cm^{-1} and the C−O stretching band at 1396 cm^{-1}, which are attributed to the acetate groups present on the ZnO particle surface. Similar observation was reported by Xiong et al.[47] for ZnO nanoparticles prepared from zinc acetate in ethanol. It can also be observed from Figure 6 that the intensity of the peak at 1724 cm^{-1} gradually decreases with increasing $Zn(Ac)_2 \cdot 2H_2O$ concentration, which can be related to the more effective interaction of β-diketone functionality with an increased amount of the deposited ZnO nanoparticles.

Preparation of hollow ZnO particles from PS/ZnO core−shell particles has been demonstrated via core dissolution by exposing them to DMSO (SEM and TEM images of hollow particles are given in the Supporting Informations, Figure S4). However, because of insufficient shell thickness (~30 nm), hollow particles could not maintain the initial spherical shape and got deformed and collapsed but were found to be unbroken. In contrast, calcination of the same composite particles at 500 °C resulted in broken shells due to the thin shell wall, similar to what has been reported by Caruso et al.[35] Neves et al.[48] described the preparation of hollow ZnO particles by deposition of hydrozincite on the polystyrene beads and subsequent calcination of prepared PS−hydrozincite composite particles at high temperature. In this approach, they reported that hollow particles maintained the shape of the template because of the deposition of a thick layer of hydrozincite but that the shell wall was not continuous. On the other hand, in our case, although the particles could not maintain the spherical shape, the shell wall was found to be continuous because of the uniform deposition of the ZnO layer.

The presence of ZnO nanoparticles on the polystyrene beads was further confirmed by X-ray photoelectron spectroscopy (XPS) experiments of composite particles. XPS spectra (Figure S3 in the Supporting Information) show the characteristic signals for zinc (Zn $2p_{3/2}$ and Zn $2p_{1/2}$ at 1022

(47) Xiong, H.-M.; Zhao, X.; Chen, J.-S. *J. Phys. Chem. B* **2001**, *105*, 10169.
(48) Neves, M. C.; Trindade, T.; Timmons, A. M. B.; Pedrosa de Jesus, J. D. *Mate. Res. Bull.* **2001**, *36*, 1099−1108.

and 1045.6 eV, respectively), oxygen (O 1s at 531.9 eV), and carbon (C 1s at 284 eV) atoms. The calculated elemental [Zn]:[C] ratio from the XPS spectra was found to be in agreement with TGA and microscopy results. (Figure S3a in the Supporting Information shows the correlation between XPS and TGA results; Figure S3b illustrates wide-scan XPS spectrum of composite particles; parts c and d of Figure S3 show the C1s spectra and Zn 2p spectrum, respectively.)

Discussion

We propose that the interaction between β-diketone groups and ZnO precursors is the driving force for the formation of PS/ZnO composite particles. It has been reported in literature[49,50] that nucleation and growth processes of ZnO nanoparticles are preceded by the formation of positively charged complexes such as $[ZnL_h(OH_2)_{N-h}]^{(2-h)+}$ (where L is an anionic ligand such as OH^- or $CH3COO^-$, etc). The β-diketone groups effectively bind with these zinc ions and provoke the nucleation and subsequent growth of ZnO nanoparticles on the surface of polystyrene beads. In the present study, we investigated the influence of reaction conditions, such as NaOH concentration, $Zn(Ac)_2 \cdot 2H_2O$ concentration, and reaction temperature on the morphology as well as the ZnO content of composite particles. Both lower NaOH concentrations (0.2 and 0.5 M) and lower reaction temperatures (40 °C) facilitate the formation of a well-defined core−shell morphology of composite particles because of the slow and controlled rate of nucleation and growth of ZnO nanoparticles. On the contrary, higher NaOH concentration (1 M) and higher reaction temperatures (55 and 70 °C) favor the "raspberry-like" morphology because of the accelerated nucleation and growth processes as well as an induced coarsening effect of ZnO nanoparticles.

A simplified process for the preparation of composite particles can be shown by Scheme 1. In the first step, the ZnO precursor interacts with the β-diketone groups of polystyrene beads and is adsorbed on their surface; in the second step, these precursors are converted in ZnO nanoparticles after reacting with NaOH. Depending on the reaction parameters, composite particles with core−shell or raspberry-like morphology are obtained.

For the precipitation of the ZnO layer on the surface of template, either the ZnO precursor or base (used as oxygen source in hydrolysis) should have a good affinity with the active sites of the template. The attachment of either onto the template surface leads to heterogeneous precipitation (precipitation on the surface of template) of ZnO nanoparticles. Moreover, it competes with the homogeneous precipitation (precipitation in solution), depending on the reaction parameters. In our study, we attempted to coat polystyrene beads with ZnO nanoparticles by capturing the ZnO precursors on the template, whereas Xia et al.[38] reported the preparation of ZnO layer on silica spheres by capturing the base. They reported the preparation of silica/ZnO core−shell particles by carrying out the hydrolysis of $Zn(Ac)_2 \cdot 2H_2O$ salt with triethanolamine in the presence of silica spheres. First, the triethanolamine was adsorbed on the surface of silica spheres by the interaction with silanol and siloxane groups; it was subsequently reacted with the ZnO precursors present in the solution, leading to the formation of ZnO layer on silica spheres.

Scheme 1. Schematic Presentation of the Synthesis of PS/ZnO Composite Particles with Raspberry and Core−Shell Morphology

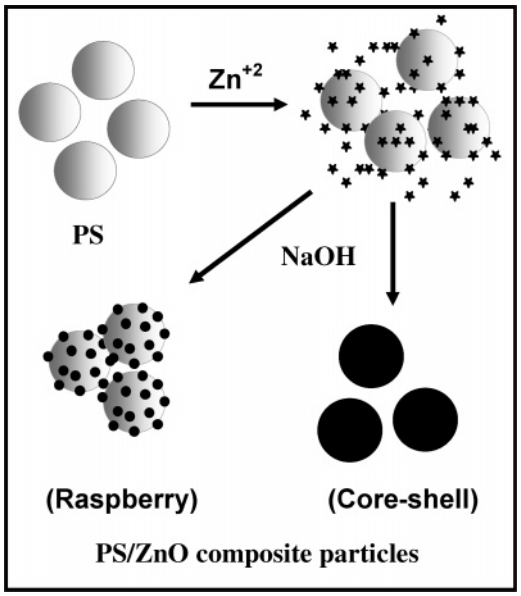

IR data prove the strong interaction between the ZnO nanoparticles and the β-diketone groups located on the polystyrene particle surface. Moreover, a change in the IR spectra of the composite particles with changing ZnO content supports this reaction mechanism described above. TGA results indicate the effective control of the reaction parameters on the ZnO content of composite particles. XRD results confirm the deposition of crystalline ZnO on the polymer beads. Removal of the PS core of core−shell composite particles via chemical dissolution resulted in unbroken but deformed hollow ZnO particles due to the thin ZnO shell.

Comparison of the present study with previous ones over the preparation of composite particles reveals that this method (a) is versatile in terms of producing composite particles with two different morphologies and (b) allows the deposition of crystalline ZnO nanoparticles on polystyrene beads, which can further extend the application of these particles. In previous studies, Chen et al.[32] reported the deposition of a silica layer and Zhong et al.[33] described the synthesis of a titanium-(di)oxide layer on the polystyrene beads, but in both cases, the deposited material was found to be amorphous.

Acknowledgment. This research was performed in frame of the SFB 287 "Reaktive Polymere" and supported by Deutsche Forschungsgemeinschaft (DFG). The authors are thankful to Mrs. E. Kern, Dr. Rudiger Hässler, and Mrs. S. Bhattacharya for helping out with SEM measurements, TGA analysis, and synthesis of polymeric particles, respectively.

(49) Tokumoto, M. S.; Pulcinelli, S. H.; Santilli, C. V.; Briois, V. *J. Sol−Gel Sci. Technol.* **2003**, *26*, 547.
(50) Brinker C. J.; Scherer, G. W. *Sol−Gel Science*; Academic Press: New York, 1989.

Supporting Information Available: SEM images of ZnO nanoparticles prepared at different temperatures and NaOH concentrations (Figure S1 and Figure S2, respectively). XPS spectra of PS/ZnO composite particles (Figure S3a shows the correlation between XPS and TGA results; Figure S3b illustrates wide-scan XPS spectrum of composite particles; parts c and d of Figure S3 show the C1s spectra and Zn 2p spectrum, respectively.) SEM and TEM images of PS/ZnO composite particles and hollow ZnO particles (Figure S4). This material is available free of charge via the Internet at http://pubs.acs.org.

CM062757G